16th World Conference on Earthquake, 16WCEE 2017

Santiago Chile, January 9th to 13th 2017

Paper N° 1523

Registration Code: S-K1462785505

PUSHOVER-BASED RISK ASSESSMENT METHOD: A PRACTICAL TOOL FOR RISK ASSESSMENT OF BUILDING STRUCTURES

M. Kosič(1), M. Dolšek(2) and P. Fajfar(3)

(1) Assistant, University of Ljubljana, Faculty of Civil and Geodetic Engineering, mirko.kosic@fgg.uni-lj.si
(2) Professor, University of Ljubljana, Faculty of Civil and Geodetic Engineering, matjaz.dolsek@fgg.uni-lj.si
(3) Professor, University of Ljubljana, Faculty of Civil and Geodetic Engineering, peter.fajfar@fgg.uni-lj.si

Abstract

The pushover-based risk assessment (PRA) method is employed, together with recently proposed dispersion values, for a practice-oriented estimation of the "failure" probabilities of reinforced concrete (RC) building structures. The test structures include a code-conforming (modern) frame, an old (non code-conforming) frame, and two code-conforming cantilever walls. The results of the PRA method are compared with the results of response history analyses performed with consideration of different levels of approximation (assessment levels), i.e. equivalent SDOF vs. MDOF response history analysis, and different ground motions sets, i.e. code-based ground motion sets vs. hazard consistent ground motion sets. In the majority of cases, the "failure" probabilities estimated with the PRA method are in between the results of more elaborate risk analyses, performed using different ground motion sets. The obtained results indicate that the old frame, which was designed and built without observing appropriate codes for seismic resistance, is exposed to at least an order of magnitude higher seismic risk than code-conforming structures. In spite of its simplicity, the PRA method was able to predict the seismic risk of the examined buildings with reasonable accuracy, thus it may become a practical tool for engineers to estimate the seismic risk of building structures.

Keywords: pushover-based risk assessment; dispersion values; RC frames; RC cantilever walls.

1. Introduction

Due to large uncertainties, the seismic performance assessment of building structures should be, in principle, based on a probabilistic approach. However, in practice, probabilistic considerations have not yet been explicitly implemented in structural design and assessment of building structures, with the exception of nuclear power plant structures. In order to facilitate a gradual introduction of probabilistic considerations into practice, some simplified practice-oriented approaches for the determination of seismic risk are needed.

Several methodologies, which allow for an explicit quantification of seismic risk in closed-form, are available [e.g. 1-3]. The computationally most demanding part of seismic risk assessment is the estimation of the fragility parameters, which is generally performed using the Incremental Dynamic Analysis − IDA [4] or the Multiple Stripe Analysis – MSA [5]. A discussion on the expected accuracy of these procedures, and suggestions on how to efficiently select the intensity levels for multiple stripe analysis (MSA) are presented in [6]. Two recently proposed risk assessment methods also rely on intensity-based assessment [7, 8]. Eads et al. [7] proposed an efficient method for estimation of seismic risk based on an initial approximation of collapse fragility curve, which is then updated using an intensity-based assessment at two intensity levels. A similar concept was also employed in the 3R method [8], which allows simple checking of the reliability of a no-collapse requirement by performing pushover analysis and few dynamic analyses for the so-called characteristic ground motions, which are scaled to a single intensity. The computational efforts increase in the case when modelling uncertainties are considered in the estimation of the fragility parameters [9]. In order to facilitate applications in practice, several simplified risk assessment methods, which allow for an approximate consideration of the effect of, both, record-to-record variability and modelling uncertainty, were developed [e.g. 10,11]. These methods combine pushover analysis of a MDOF system and response history analysis of an equivalent SDOF system. A further simplification represents the Pushover-based Risk Assessment (PRA) method [12], which does not require any response history analysis. By combining the SAC-FEMA method [2], which permits probability assessment in closed form, and the pushover-based N2 method [13], which is used for the determination of the capacity of the structure, an explicit equation for the quick estimation of the annual probability of “failure” of a structure was derived [12], which is appropriate for practical applications, provided that predetermined default values for dispersions are available. Such values were recently proposed based on extensive numerical studies [14], and can be used for pushover-based risk assessment of reinforced concrete frames and cantilever walls.

In this paper, the PRA method is employed for the estimation of the “failure” probabilities of four selected reinforced concrete (RC) structures, and its results are compared with the results of response history analyses performed with consideration of different levels of approximation (assessment levels), i.e. equivalent SDOF vs. MDOF response history analysis, and different ground motions sets, i.e. code-based ground motion sets vs. hazard consistent ground motion sets.

2. Methodology

2.1 Pushover-based risk assessment (PRA) method

The “failure” probability of building structures, i.e. the probability of exceeding the near-collapse limit state (NC), which is assumed to be related to an economic failure of a structure, can be estimated as [1, 12]

$$P_{NC} = \exp\left[0.5\, k^2\, \beta_{NC}^2\right] H(\tilde{S}_{a,NC}) = \exp\left[0.5\, k^2\, \beta_{NC}^2\right] k_0\, \tilde{S}_{a,NC}^{-k}, \tag{1}$$

where the parameters $\tilde{S}_{a,NC}$ and β_{NC} are the fragility parameters, i.e. the median and the logarithmic standard deviation of the NC limit-state spectral accelerations due to record-to-record variability and modelling uncertainty, and the parameters k and k_0 are the slope and the intercept of the hazard curve in log-to-log domain. It is assumed that the fragility function has a lognormal distribution and that the hazard curve is linear in the logarithmic domain. The median near collapse limit-state acceleration ($\tilde{S}_{a,NC}$) is estimated using the N2 method [13], whereas predetermined dispersion values are used for approximate consideration of the record-to-record variability and modelling uncertainty, which cannot be directly simulated by the N2 method. It should be noted that, as opposed to the original formulation of the PRA method [12] which uses PGA as the intensity measure, the spectral acceleration at period of the equivalent SDOF model ($S_a(T^*)$) was used as the intensity measure in the presented study.

A widely accepted definition of the near collapse limit state is still not available. In this paper we assumed that the NC limit state corresponds to 80% strength at the softening branch of the pushover curve. An alternative definition can be the NC limit state of the most critical vertical element.

First, the pushover analysis with an invariant distribution of lateral forces is performed, and the pushover curve is idealized with a bilinear relationship. The relations of the N2 method [13] are used for the calculation of the MDOF-SDOF transformation factor Γ and the characteristics of the equivalent SDOF model, i.e. the mass m^*, the yield displacement D_y^*, the yield force F_y^*, the period T^*, and the yield spectral acceleration S_{ay}:

$$\Gamma = \frac{m^*}{\sum m_i\, \Phi_i^2}, \quad m^* = \sum m_i\, \Phi_i, \quad D_y^* = \frac{D_y}{\Gamma}, \quad F_y^* = \frac{F_y}{\Gamma}, \quad T^* = 2\pi\sqrt{\frac{m^*\, D_y^*}{F_y^*}}, \quad S_{ay} = \frac{F_y^*}{m^*}, \tag{2}$$

where D_y and F_y are the yield displacement and yield force of the MDOF system, respectively. Next, the failure ductility μ_{NC} is calculated as the ratio of the failure displacement D_{NC} and the yield displacement of the structure D_y. The failure capacity $\tilde{S}_{a,NC}$ is calculated as the product of the yield spectral acceleration S_{ay} and the reduction factor due to ductility R_μ, which is a function of the failure ductility μ_{NC} and period T^*:

$$\tilde{S}_{a,NC} = S_{ay}\, R_\mu(\mu_{NC}, T^*); \quad R_\mu = \begin{cases} (\mu_{NC} - 1)\,\dfrac{T^*}{T_C} + 1 & T^* \le T_C \\ \mu_{NC} & T^* > T_C \end{cases} \tag{3}$$

In the last step, the calculated failure capacity is combined with appropriate dispersions of failure capacity β_{NC} (see Section 2.2) and parameters of seismic hazard curve (k and k_0) for the estimation of the failure probability using Eq. (1). The parameters k and k_0 are estimated by fitting the seismic hazard curve with a linear function in logarithmic domain. In absence of more reliable data, the procedure proposed in [12] can be used. Please consult the Appendix, where a summary of all the steps of the PRA method is presented for a selected example.

2.2 Dispersions for pushover-based risk assessment

Table 1 presents the dispersion values for the pushover-based risk assessment of reinforced concrete (RC) frames and cantilever walls, which were recently proposed based on extensive numerical studies of typical structures [14]. In this paper, only the values calculated for the near-collapse limit state, and with consideration of, both, record-to-record variability and modelling, are employed ($\beta_{NC,RU} \equiv \beta_{NC}$). The dispersion due to only record-to-record variability ($\beta_{LS,R}$) and only modelling uncertainty ($\beta_{LS,U}$), and the values for the collapse limit state, can be found in [14].

Table 1 – Dispersion values for the pushover-based risk assessment of code-conforming frames, old (non code-conforming) frames, and code-conforming cantilever walls.

	Code-conforming frames	Old frames		Code-conforming cantilever walls
		Majority	Soft-storey and invariant PM	
$\beta_{NC,RU}$	0.45	0.45	0.30	0.55

The performed studies indicated that the dispersions due to record-to-record variability ($\beta_{LS,R}$) are related to the ductility demand, which is closely related to the period elongation due to the formation of damage (see Fig. 1a), whereas the dispersions due to modelling uncertainty ($\beta_{LS,U}$) depend on the period of the structure (T^*), which influences the curvature of the IDA curves. From Fig. 1b, it can be seen that the record with a larger curvature of the IDA curve, i.e. the record *r*2, yields a smaller dispersion $\beta_{LS,U}$. Short-period structures ($T^*<T_c$) tend to have, on average, a larger curvature of IDA curves, which produces lower dispersions ($\beta_{LS,U}$) (see [14] for details).

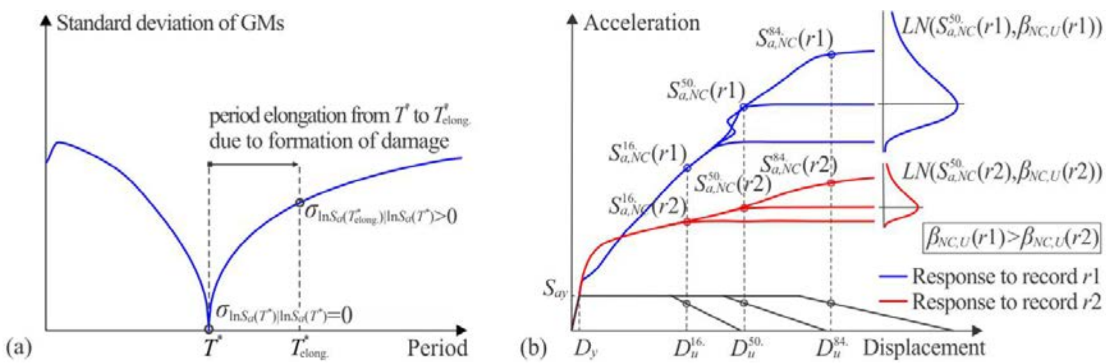

Fig. 1 – Schematic presentation of the influence of (a) the period elongation due to formation of damage on the increase of input record-to-record variability, and (b) the curvature of the IDA curve on the calculated dispersions $\beta_{LS,U}$ for a SDOF model with uncertain deformation capacity, subjected to two ground motions.

2.3 Seismic risk assessment based on the response history analysis with consideration of record-to-record variability and modelling uncertainty

For comparison reasons, the seismic risk of the examined structures was also calculated by more advanced methods based on response history analysis. Two existing procedures, i.e. [10] and [9], which enable consideration of record-to-record variability and modelling uncertainty, were used. The flowcharts of the procedures, which will be referred to as assessment levels 1 and 2, are presented in Fig. 2.

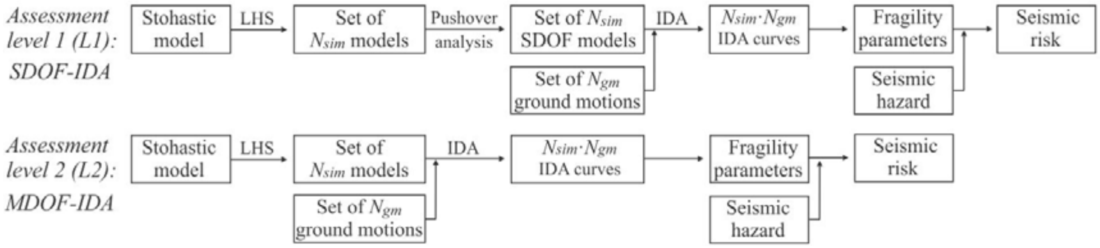

Fig. 2 –Seismic response assessment based on assessment level 1 (L1) and assessment level 2 (L2).

The first step of both assessment levels is the development of the stochastic structural model. A set of structural models is than generated by Latin Hypercube Sampling (LHS) based on the selected probability distributions and correlations between random variables. The same algorithm for LHS [15] is employed at both assessment levels. The estimation of the fragility parameters involves nonlinear response history analyses, which allow consideration of the effects of record-to-record variability and modelling uncertainty that are, respectively, captured by an appropriate set of N_{gm} ground motions and by a set of N_{sim} structural models. In the case of the assessment level 1, the fragility parameters are evaluated based on pushover analysis and subsequent nonlinear response history analysis of the set of N_{sim} equivalent SDOF models, whereas in case of assessment level 2, the nonlinear response history analysis are performed directly for the set of N_{sim} structural models. For each of the N_{sim} structural models (or SDOF models), the intensity of the ground motions is gradually increased until the near collapse limit state is attained [4]. The result is a sample of near collapse spectral accelerations $S_{a,NC}(r,u)$ of size $N_{sim} \cdot N_{gm}$, which is employed for the estimation of the fragility parameters using the equations:

$$\tilde{S}_{a,NC} = e^{\frac{1}{N_{sim} \cdot N_{gm}} \sum_{r=1}^{N_{gm}} \sum_{u=1}^{N_{sim}} \ln\left(S_{a,NC}(r,u)\right)}, \qquad (4)$$

$$\beta_{NC}^2 = \frac{1}{N_{sim} N_{gm}} \sum_{r=1}^{N_{gm}} \sum_{u=1}^{N_{sim}} \left(\ln\left(S_{a,NC}(r,u)\right) - \ln\left(\tilde{S}_{a,NC}\right)\right)^2,$$

where N_{gm} is the number of ground motions used in the analysis, N_{sim} is the number of simulations based on the Monte Carlo simulations with LHS, and r and u denote the rth ground motion and uth structural model (or SDOF model), respectively. In the last step, the calculated fragility parameters are combined with seismic hazard information, and are used for the estimation of the seismic risk with Eq. (1).

3. Case study - comparison of “failure” probabilities for selected examples using approaches of different level of accuracy and different ground motion sets

3.1 The investigated structures and structural modelling

The investigated group of structures consists of a code-conforming frame, an old (non code-conforming) frame, and two code-conforming cantilever walls (see Fig. 3). The structures were already employed in previous studies by the authors [11, 14], where references and additional details can be found. It should be noted that, for simplicity, the frames were analysed independently in two main directions (X and Y, see Fig. 3).

The structural models were created using the PBEE toolbox [16], which allows a rapid generation of nonlinear models for OpenSees [17]. The floor diaphragms were assumed to be rigid in their plain, and the masses and moments of inertia of each floor were lumped at the centre of gravity. The beams and the columns were modelled with elastic elements and rotational plastic hinges at both ends. In the case of the cantilever walls, elastic elements were placed over the height of the wall, and a single plastic hinge was assumed at their base. Moment-rotation envelopes were modelled according to the principles described in a previous study [18]. The ultimate rotations in the columns at the near collapse (NC) limit state, which corresponds to 80% of the maximum moment in the post-capping region, were estimated by the conditional average estimator − CAE method [19]. On the other hand, the EC8-3 [20] formula for secondary elements (γ_{el} = 1.0, representing mean estimates) was employed for the calculation of the ultimate rotations in the beams and walls. Due to the lack of seismic detailing and the use of smooth bars, the computed ultimate rotations for the old frame were multiplied by a factor of 0.667 [11]. For the old frame, the impact of potential shear failures of the columns was also taken into account. In the assessment level 1, the shear failures of the columns were approximately taken into account using the iterative pushover analysis − IPP [21], whereas in the case of the assessment level 2, which is based on response history analysis, the concept of “element removal” proposed in [22], was employed. The flexural strength at both ends of the columns (and in both directions) was distributed between two plastic hinges placed in parallel, and the shear demand-capacity ratio was monitored in each step of the analysis. In the case that a shear failure of a column was detected, one of the hinges was removed from the model and the analysis was continued with consideration of a reduced moment-rotation envelope. In this study, an arbitrary 60% drop of flexural strength after occurrence of a shear failure was assumed. At both assessment levels, the mean values of shear strength of the columns were estimated according to the EC8-3 [20] formula (γ_{el} = 1.0).

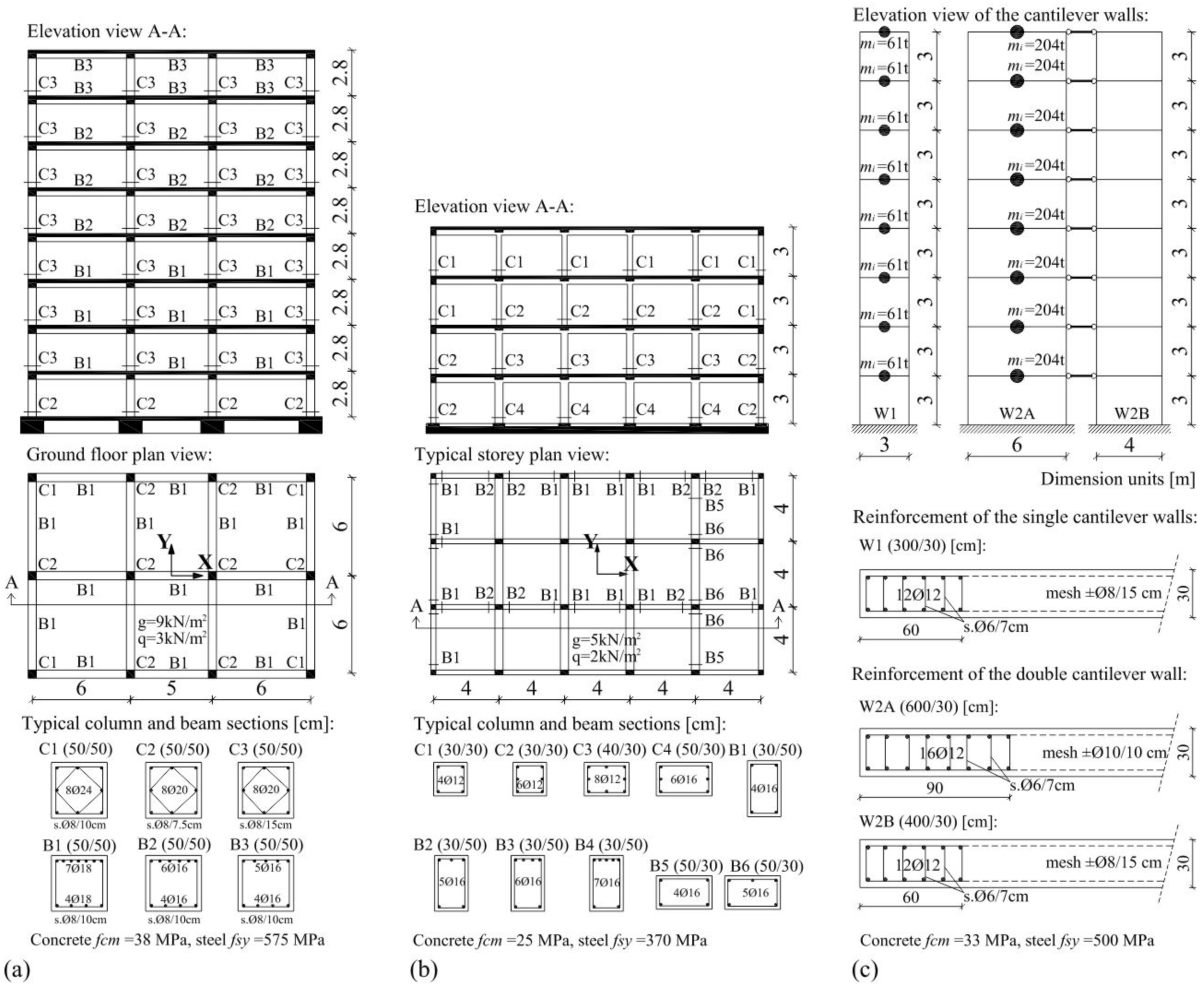

Fig. 3 – (a) Elevation view, plan view and reinforcement layout of the 8-storey code-conforming frame, (b) elevation view, plan view and reinforcement layout of the 4-storey old (non code-conforming frame), and (c) elevation view and reinforcement layout of the 8-storey single and double code-conforming cantilever walls.

Nonlinear response history analyses were performed considering the hysteretic behaviour of the components of the structural model, and that of the SDOF model, according to the principles implemented in the "uniaxial hysteretic material" available in OpenSees [17], and Rayleigh damping proportional to mass and instantaneous stiffness (5% in the first two modes). The *P*-Δ effect due to gravity loads was taken into account in all the analyses. Additional details regarding the structural modelling can be found in [16].

3.2 Ground motion selection and ground motion sets

For each of the examined structures, two sets of 30 ground motions were selected from the PEER NGA database [23] in such a way that the mean and standard deviation of horizontal acceleration spectra matched, respectively, two predefined target spectra, and the corresponding conditional standard deviations. A comparison of the ground motion sets, selected for the analysis of the 8-storey code-conforming frame, is presented in Fig. 4. The first set of ground motions (denoted S1) was selected to match the elastic spectrum according to Eurocode 8 [24] for soil type C with a peak ground acceleration of 0.29 *g* (see Fig. 4a), and a conditional standard deviation (see Fig. 4b). The second set of ground motions was selected according to the conditional spectrum approach [25] (denoted S2, see Fig. 4a), by taking into account the results of the disaggregation of seismic hazard for Ljubljana (Slovenia). The return periods 10,000 years and 2,475 years were assumed for the conditional spectra to be used for the analysis of the code-conforming and the old structures, respectively. Ground motion selection was performed according to the procedure [26]. Additional details regarding the ground motion selection can be found in [14].

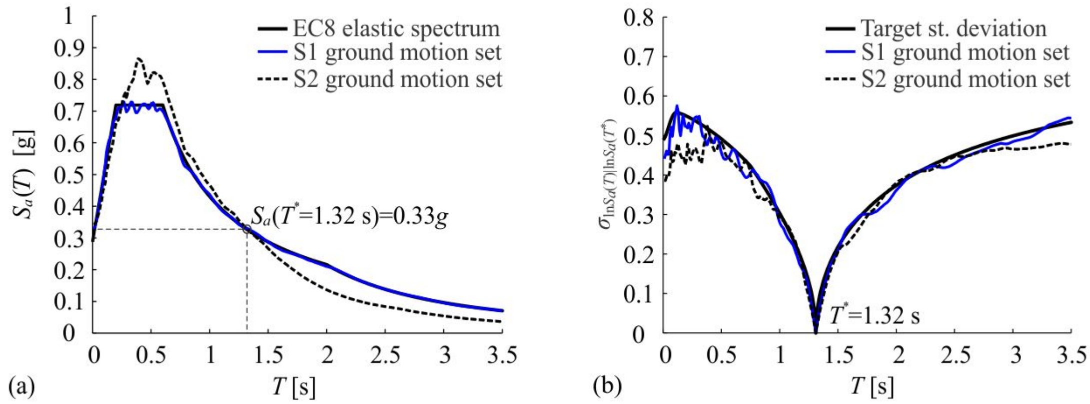

Fig. 4 – Comparison of (a) the mean spectra and (b) the standard deviation of the spectra for the ground motions sets S1 and S2, normalized to the spectral acceleration =0.33 g based on the Eurocode 8 (EC8) spectrum for PGA=0.29 g, for the example of the 8-storey code-conforming frame.

3.3 Input random variables used for simulation of modelling uncertainty

The statistical characteristics of the input random variables, used for the simulation of modelling uncertainty at the assessment levels 1 and 2, are presented in Table 2. The mean/median values of random variables are not included in Table 2, since these values vary between structures, and even between individual elements within a structure. The references for the assumed statistical characteristics and additional details can be found in a previous study by the authors [11].

Table 2 –Statistical characteristics of the input random variables

Variable		CV	Distribution
storey mass	m_i	0.10	normal
concrete strength	f_{cm}	0.20	normal
steel yield stress	f_{sy}	0.05	lognormal
effective slab width	b_{eff}	0.20	normal
yield rotation of the columns	$\Theta_{y,c}$	0.36	lognormal
yield rotation of the beams	$\Theta_{y,b}$	0.36	lognormal
yield rotation of the walls	$\Theta_{y,w}$	0.36	lognormal
ultimate rotation of the columns – CAE	$\Theta_{u,c}$	0.40	lognormal
ultimate rotation of the beams – EC8-3	$\Theta_{u,b}$	0.60	lognormal
ultimate rotation of the walls – EC8-3	$\Theta_{u,w}$	0.60	lognormal
system damping, 5%	ξ	0.40	normal
shear strength model	V_R	0.15	normal
ultimate rotation at shear failure	$\Theta_{u,c,s}$	0.35	lognormal

3.4 The "failure" probabilities for the selected examples, and discussion of the results

The first step of the PRA method is the pushover analysis of the examined structures. The obtained pushover curves are idealized with a bilinear relationship (see Fig. 5a). Using Eq. (2), the following characteristics of the equivalent SDOF models were obtained for the code conforming frame (X and Y), the old frame (X and Y), and the two cantilever walls, respectively: T^*=[1.32; 1.37; 0.66; 1.02; 1.65; 0.93] s, S_{ay}=[0.14; 0.14; 0.17; 0.12; 0.08; 0.21] g, and μ_{NC}=[7.5; 7.0; 3.7; 6.1; 8.5; 7.9]. These results are used for the simplified estimation of the failure capacity with Eq. (3). Appropriate dispersions β_{NC} were than assumed based on the values presented in Table 1. For the code-conforming frame and the cantilever walls, the dispersions β_{NC}=0.45 and β_{NC}=0.55 were employed. In the case of the old frame, the pushover analysis in X direction indicated a soft storey mechanism (see Fig. 5b). Due to the soft storey mechanism and a low value of the maximum normalized axial force in the columns ($\nu_{\max} = 0.12 \le 0.25$), the frame in X direction was categorized as not sensitive to variation of the plastic mechanism due to the effect of modelling uncertainty (invariant plastic mechanism) [11], and a lower dispersion was assumed β_{NC} =0.30. On the contrary, the pushover analysis in the Y direction indicated a global plastic mechanism. Consequently, the dispersion value proposed for the majority of old frames, i.e. β_{NC} =0.45, was assumed for the analysis in Y direction. Finally, the mean annual probabilities of "failure" (P_{NC}) were calculated according to Eq.(1), assuming a typical slope of the seismic hazard curve k=3. The parameter k_0 was calculated for each building from the spectral acceleration corresponding to a 475-years design event [12], considering the Eurocode's elastic acceleration spectrum [24] presented in section 3.2. Note that the step-by-step procedure for estimation of the "failure" probability of the code-conforming frame (Y direction) is presented in the Appendix.

In Table 3, the fragility parameters $\tilde{S}_{a,NC}$ and β_{NC}, mean annual probabilities of failure (P_{NC}), and failure probabilities in 50 years ($P_{NC}^{50} = 1-\left(1-P_{NC}\right)^{50}$) obtained by the PRA method were compared with those obtained based on nonlinear response history analyses with consideration of two assessment levels (L1 and L2), and two ground motion sets (S1 and S2). For the examined structures, a quite good agreement of the results between both assessment levels was observed. It seems that the ground motion set used for response history analysis had a larger influence on the results than the calculation procedure. The N2 method, in general, overestimated the median near collapse intensities in comparison to those obtained with the ground motion sets S1. The observed differences are mainly due to the simplified estimation of the failure capacity, and neglecting the influence of modelling uncertainties on the median values, which do not only increase the dispersion of the response, but can also lower the limit-state intensity [27, 10]. On the other hand, when compared with the S2 values, the estimated $\tilde{S}_{a,NC}$ values using the N2 method are always on the safe side, i.e. they are underestimated, on average, by 15 %.

Table 3 – Comparison of fragility parameters $\tilde{S}_{a,NC}$ and β_{NC}, mean annual probabilities of failure P_{NC}, and failure probabilities in 50 years (P_{NC}^{50}), as obtained by the Pushover-based Risk Assessment (PRA) method and nonlinear response history analyses with assessment levels 1 and 2 (L1 and L2), considering ground motions (GM) sets selected according to the Eurocode 8 elastic spectrum (S1) and the conditional spectrum (S2).

PRA vs. L1 (GM sets S1 and S2)	$\tilde{S}_{a,NC}$ $[g]$			β_{NC}			P_{NC} $[10^{-4}]$			P_{NC}^{50} [%]		
	PRA	S1	S2	PRA	S1	S2	PRA	S1	S2	PRA	S1	S2
Code-conforming frame X	1.05	0.84	1.27	0.45	0.45	0.45	1.6	3.1	0.9	0.8	1.5	0.4
Code-conforming frame Y	0.95	0.80	1.18	0.45	0.45	0.46	1.9	3.2	1.0	0.9	1.6	0.5
Old frame X *	0.63	0.49	0.69	0.30	0.33	0.39	35.2	81.5	35.4	16.2	33.6	16.3
Old frame Y	0.74	0.51	0.79	0.45	0.41	0.42	9.8	25.6	7.1	4.8	12.0	3.5
Single cantilever wall	0.67	0.68	0.91	0.55	0.56	0.59	4.9	4.9	2.4	2.4	2.4	1.2
Double cantilever wall	1.66	1.17	1.88	0.55	0.5	0.56	1.8	4.0	1.3	0.9	2.0	0.7

PRA vs. L2 (GM sets S1 and S2)	$\tilde{S}_{a,NC}$ $[g]$			β_{NC}			P_{NC} $[10^{-4}]$			P_{NC}^{50} [%]		
	PRA	S1	S2	PRA	S1	S2	PRA	S1	S2	PRA	S1	S2
Code-conforming frame X	1.05	0.91	1.31	0.45	0.41	0.40	1.6	2.1	0.7	0.8	1.0	0.3
Code-conforming frame Y	0.95	0.86	1.22	0.45	0.42	0.42	1.9	2.3	0.8	0.9	1.1	0.4
Old frame X *	0.63	0.56	0.75	0.30	0.35	0.41	35.2	58.0	29.7	16.2	25.3	13.8
Old frame Y	0.74	0.52	0.72	0.45	0.39	0.41	9.8	22.4	9.1	4.8	10.6	4.4
Single cantilever wall	0.67	0.72	0.93	0.55	0.52	0.55	4.9	3.4	1.8	2.4	1.7	0.9
Double cantilever wall	1.66	1.28	2.06	0.55	0.51	0.53	1.8	3.2	0.8	0.9	1.6	0.4

* A soft storey mechanism was obtained based on the pushover analysis.

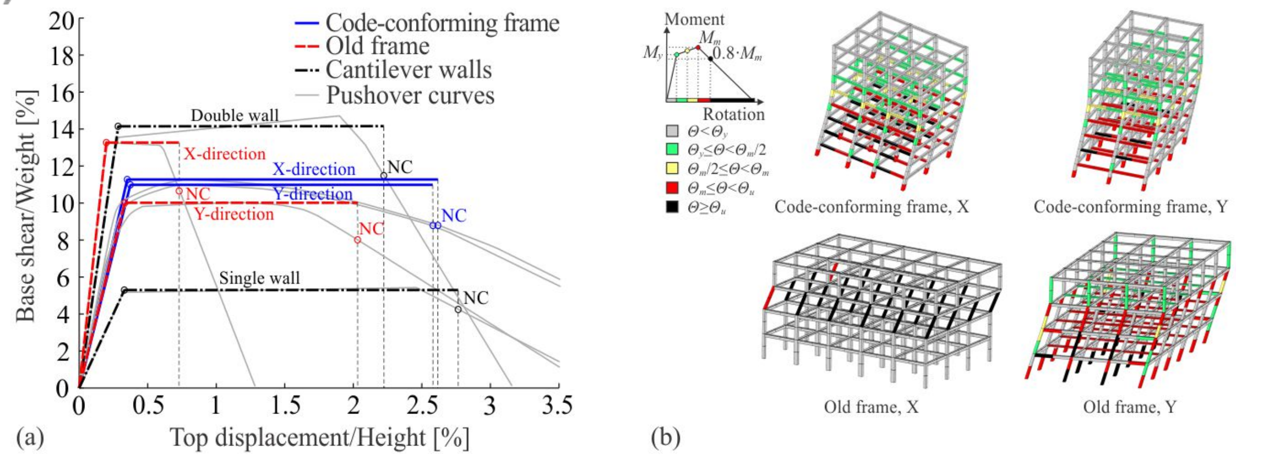

Fig. 5 – (a) The pushover curves and idealized pushover curves for the examined structures, and (b) the plastic mechanisms and corresponding damage in the plastic hinges at near collapse limit (NC) for the frame structures.

The dispersion values, employed in the PRA method, match the results of both assessment levels relatively well. The differences in β_{NC} values are usually within 10 %. In the majority of cases, the dispersions employed in the PRA method slightly overestimate the dispersion in comparison to assessment levels 1 and 2, especially in the case of the ground motion set S1. The only exception to this is the old frame with a soft storey mechanism (X direction), for which the dispersion β_{NC} is underestimated by about 10 % and 25 % when compared with the results of the response history analyses performed with ground motion sets S1 and S2, respectively.

The comparison of failures probabilities indicated that the PRA was able to provide, in the majority of cases, estimates of seismic risk in between the results obtained by response history analysis with consideration of ground motions selected using two extreme alternatives in terms of the possible target spectra used for ground motion selection, i.e. a code-based (uniform hazard) spectrum vs. a conditional spectrum. A similar conclusion can be drawn from Fig. 6, which presents a comparison of the percentile IDA curves between assessment levels 1 and 2, and between ground motions sets S1 and S2. For the presented examples, the IN2 curves were always in between the 50th percentile (median) IDA curves corresponding to the S1 and S2 ground motion sets. The employment of ground motion set S2 resulted in a significantly larger capacity of the structures compared with the set S1 (see Fig. 6), since the conditional spectrum produces a lower seismic demand for the periods larger than T^*, in comparison to the Eurocode 8 elastic spectrum (see Fig. 4a). If compared to S2, the S1 values of $\tilde{S}_{a,NC}$ are underestimated by about 30 % to 40 %, whereas the dispersions β_{NC} are underestimated by 5 % to 10 %. As a result, the S1 failure probabilities are overestimated in comparison with the ground motion set (S2).

The obtained results also indicated that, for the examined structures, the level of assessment employed, i.e. L1 or L2, did not have significant influence on the calculated failure probabilities. In general, the employment of the assessment level 1 (L1), which is based on the pushover analysis, resulted in about 30 % overestimated failures probabilities. This was due to 5 to 10 % underestimated $\tilde{S}_{a,NC}$ values, and about 5 % overestimated dispersions β_{NC}. In Fig. 6 it can be seen that the differences in the dispersions between assessment levels can be attributed mainly to the differences in the 16th percentile IDA curves. This is due to the formation of higher failure modes at seismic intensities near the 16th percentile IDA curve [28], which cannot be simulated with the standard pushover analysis taking into account only the fundamental mode.

Considering the simplifying assumptions introduced in this study, especially in the definition of the seismic hazard, the failure probabilities of code-conforming structures were in order of $1\cdot10^{-4}$ and $2\cdot10^{-4}$ per year (between 0.5 % and 1 % in 50 years). The computed failure probabilities are in line with the results of previous studies [12]. It should be noted, however, that absolute values of failure probabilities are sensitive to the input data and simplifying assumptions made. On the other hand, comparisons between structures are more reliable, and provide additional data for decision making. The results presented in Table 3 demonstrate that the old frame is exposed to at least an order of magnitude larger seismic risk than the code-conforming structures. Seismic risk was especially high in the X direction, where a soft storey mechanism is expected.

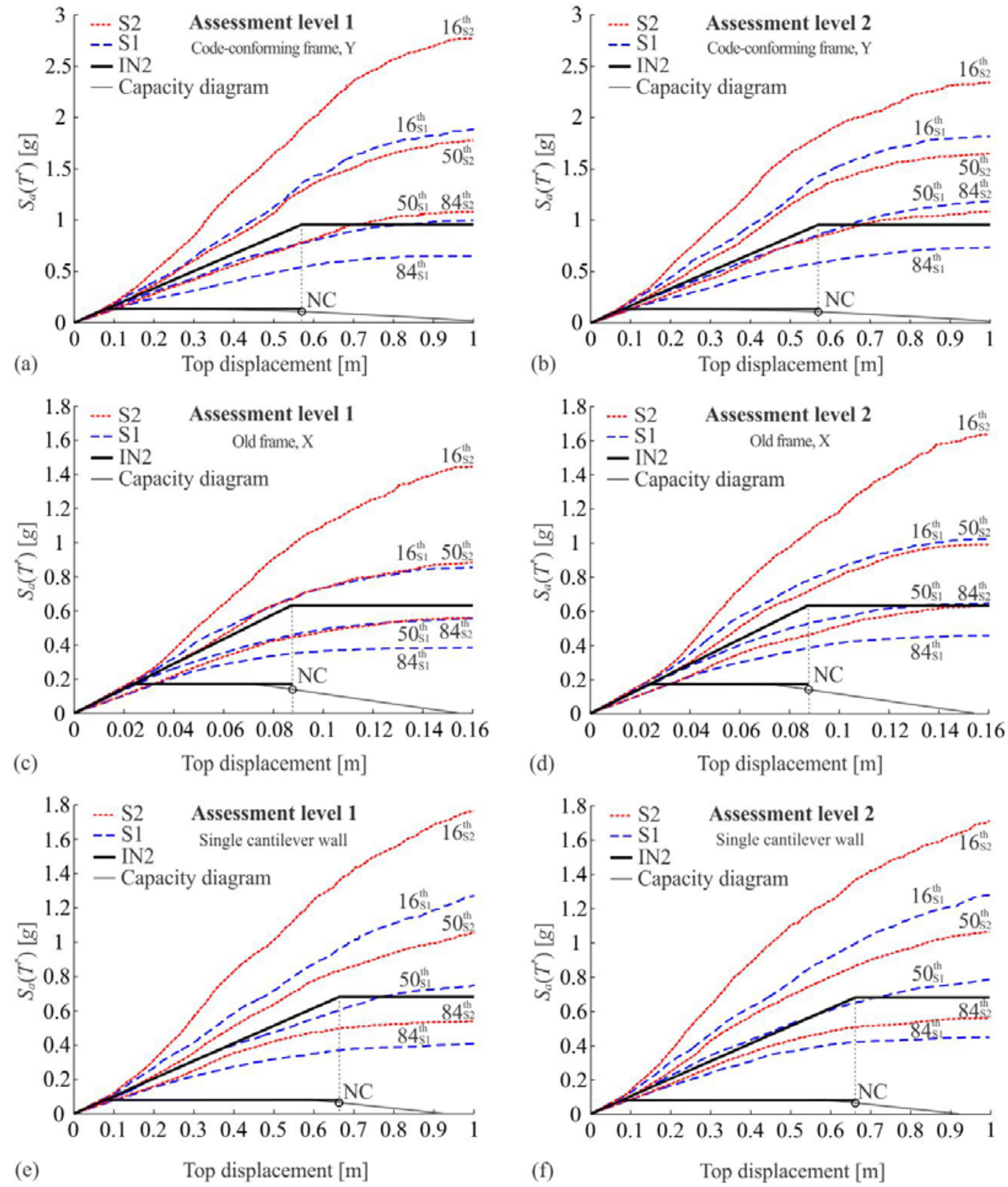

Fig. 6 – Comparison of the percentile IDA curves between assessment levels 1 and 2, determined for ground motions sets S1 and S2, for the (a,b) code-conforming frame in Y direction, (c,d) the 4-storey old frame in X direction, and (e,f) the single cantilever wall.

4. Conclusions

The paper presents an application of the pushover-based risk assessment (PRA) method for the estimation of "failure" probabilities, i.e. probabilities of exceeding the near collapse limit state, for the examples of four RC building structures. The method was employed together with recently proposed default dispersion values. The results of the PRA method were compared with the results of response history analyses performed with consideration of different levels of approximation (assessment levels), i.e. equivalent SDOF vs. MDOF response history analysis, and different ground motions sets, i.e. code-based ground motion sets vs. hazard consistent ground motion sets, which were selected according to the conditional spectrum.

The obtained results indicated that the PRA was able to provide, in the majority of cases, estimates of failure probabilities in between the results of more elaborate risk analyses, performed by using two extreme alternatives in term of ground motion sets for seismic response assessment. The dispersion values, employed in the PRA method, matched the results of more elaborate analyses relatively well. Especially good was the agreement with the results obtained with the code-based ground motions sets.

For the examined structures, the level of approximation employed in the response history analyses had only a moderate influence of the calculated failure probabilities. This indicates that the seismic response of the examined structures was predominantly affected by the first vibration mode, which is the basic assumption of all pushover methods, including the PRA method.

The old building, which was designed and built without observing appropriate codes for seismic resistance, was shown to be exposed to at least an order of magnitude higher seismic risk than code-conforming structures. Extremely high seismic risk was estimated for the direction in which a soft storey mechanism is likely to occur. The results of this study demonstrate that the PRA method is, in spite of its simplicity, able to predict the seismic risk of low- to medium-rise building structures with reasonable accuracy, thus it may become a practical tool for engineers.

5. Acknowledgements

The results presented in this paper are based on work that has been continuously supported by the Slovenian Research Agency (J2-4180, P2-0185). This support is gratefully acknowledged.

6. Appendix: Step-by-step estimation of the "failure" probability with the PRA method

The appendix presents the required steps for the estimation of the "failure" probability, i.e. probability of exceeding the near-collapse limit state (NC), of a structure using the PRA method. The example of the 8-storey code-conforming frame (Y direction, Fig. 3) is employed in this demonstration. The shape of the Eurocode 8 Type 1 spectrum [24] for soil type C is assumed in the computations.

I. Input data

(a) The mathematical model of the structure suitable for pushover analysis;
(b) Data on the dispersion of the failure capacity;
(c) The linearized seismic hazard curve for $S_a(T^*)$ at the location of the building ($H = k_0 S_a^{-k}$).

II. Pushover analysis and the parameters of the equivalent SDOF model (Fig. A.1a)

(a) Pushover analysis with an invariant pattern of lateral forces: $P_i = m_i \Phi_i$;
(b) Estimation of the NC limit state (e.g. strength decreases to 80% of the maximum strength or NC limit state is reached in the first critical vertical element). For more details see Section 2.1;
(c) Bilinear idealization of the pushover curve;
(d) Determination of the characteristics of the equivalent SDOF model: force-displacement relationship (F^* - D^*), the mass (m^*), the period (T^*) and the yield spectral acceleration (S_{ay}).

III. Estimation of the capacity at "failure" with the N2 method (Fig. A.1b)

(a) Calculation of the failure ductility: $\mu_{NC} = D_{NC} / D_y = 7.0$
(b) Calculation of the reduction factor R_μ using the relations in [13]: for $T^* > T_C$: $R_\mu = \mu_{NC}$
(c) Calculation of the failure capacity: $\tilde{S}_{a,NC} = S_{ay} R_\mu = 0.137\, g \cdot 7.0 = 0.95\, g$. The corresponding peak ground acceleration amounts to $\tilde{a}_{g,NC} = 0.87\, g$.

IV. Assumption of the dispersion of "failure" capacity

(a) For the code-conforming frame the value $\beta_{NC} = 0.45$ is used (Table 1, see section 2.2).

V. Estimation of the seismic hazard parameters

(a) In the absence of more reliable data, a typical slope of the seismic hazard curve k=3 is assumed.
(b) Elastic Eurocode 8 spectrum for soil type C is used, with PGA=0.29 g and $S_a(T = 1.37)$ =0.31 g for 475 years return period: $k_0 = 1/\left(475 \cdot S_a^{-k}\right) = 6.27 \cdot 10^{-5}$ (see e.g. [12]).

VI. Estimation of the "failure" probability

(a) Using Eq. (1), the mean annual probability of "failure" $P_{NC} = 1.9 \cdot 10^{-4}$ is obtained, which is equivalent to a "failure" probability in 50 years of $P_{NC}^{50} = 1 - \left(1 - P_{NC}\right)^{50} = 0.9\,\%$.

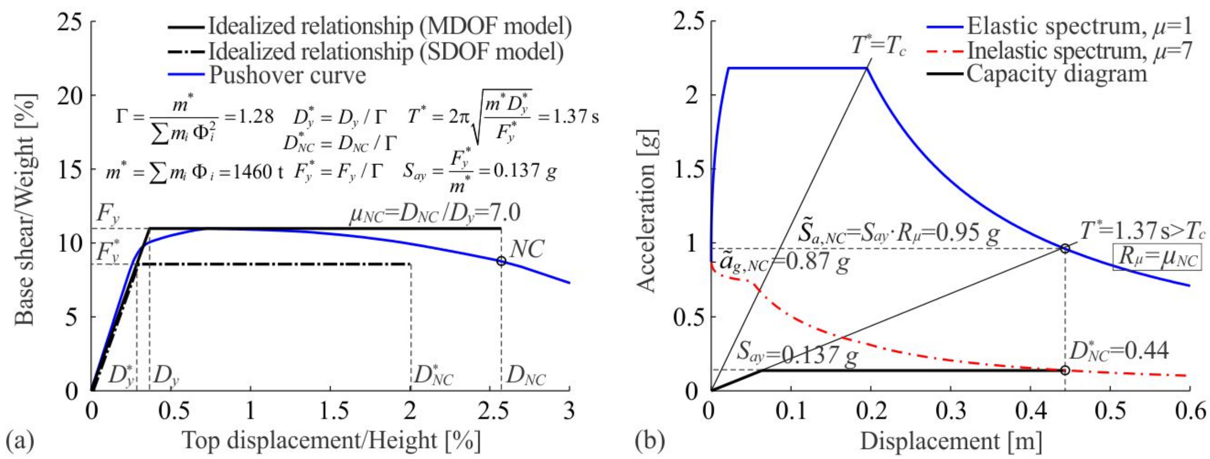

Fig. A.1 – (a) The pushover curve, and the idealized force-displacement relationship of the MDOF and equivalent SDOF model, and (b) elastic and inelastic demand spectra (corresponding to NC limit state), and the capacity diagram in acceleration-displacement (AD) format, for the 8-storey code-conforming frame (Y direction) – the weight and height of the structure are, respectively, W=22800 kN and H=22.15 m.

7. References

[1] Cornell CA (1996): Calculating building seismic performance reliability: a basis for multi-level design norms. *Eleventh World Conference on Earthquake Engineering*, Mexico City, Mexico.

[2] Cornell CA, Jalayar F, Hamburger RO, Foutch DA (2002): Probabilistic basis for 2000 SAC Federal Emergency Management Agency Steel Moment Frame Guidelines. *Journal of Structural Engineering ASCE*, **128** (4), 526-533.

[3] Lazar N, Dolšek M (2014): A closed form solution for seismic risk assessment incorporating intensity bounds. *Engineering structures*, **78**, 78-89.

[4] Vamvatsikos D, Cornell CA (2002): Incremental dynamic analysis. *Earthquake Engineering and Structural Dynamics*, **31** (3), 491-514.

[5] Jalayer F, Cornell CA (2009): Alternative non-linear demand estimation methods for probability-based seismic assessments. *Earthquake Engineering and Structural Dynamics*, **38** (8), 951-972.

[6] Baker JW (2015): Efficient analytical fragility function fitting using dynamic structural analysis. *Earthquake Spectra*, **31** (1), 579-599.

[7] Eads L, Miranda E, Krawinkler H, Lignos DG (2013): An efficient method for estimating the collapse risk of structures in seismic regions. *Earthquake Engineering and Structural Dynamics*, **42** (1), 25-41.

[8] Dolšek M, Brozovič M (2016): Seismic response analysis using characteristic ground motion records for risk-based decision making. *Earthquake Engineering and Structural Dynamics*, **45** (3), 401-420.

[9] Dolšek M (2009): Incremental dynamic analysis with consideration of modeling uncertainties. *Earthquake Engineering and Structural Dynamics*, **38** (6), 805-825.

[10] Dolšek M (2012): Simplified method for seismic risk assessment of buildings with consideration of aleatory and epistemic uncertainty. *Structure and Infrastructure Engineering*, **8** (10), 939-953.

[11] Kosič M, Fajfar P, Dolšek M (2014): Approximate seismic risk assessment of building structures with explicit consideration of uncertainties. *Earthquake Engineering and Structural Dynamics*, **43** (10), 1483-1502.

[12] Fajfar P, Dolšek M (2012): A practice-oriented estimation of the failure probability of building structures. *Earthquake Engineering and Structural Dynamics*, **41** (3), 531-547.

[13] Fajfar P (2000): A nonlinear analysis method for performance-based seismic design. *Earthquake Spectra*, **16** (3), 573-592.

[14] Kosič M, Dolšek M, Fajfar P (2016): Dispersions for pushover-based risk assessment of reinforced concrete frames and cantilever walls. *Earthquake Engineering and Structural Dynamics.* DOI: 10.1002/eqe.2753.

[15] Vořechovský M, Novák D (2009): Correlation control in small-sample Monte Carlo type simulations I: A simulated annealing approach. *Probabilistic Engineering Mechanic*s, **24** (3), 452-462.

[16] Dolšek M (2010): Development of computing environment for the seismic performance assessment of reinforced concrete frames by using simplified nonlinear models. *Bulletin of Earthquake Engineering*, **8** (6), 1309-1329.

[17] Open system for earthquake engineering simulation (OpenSees). Pacific Earthquake Engineering Research Center, 2013. Available from: http://opensees.berkeley.edu.

[18] Fajfar P, Dolšek M, Marušić D, Stratan A (2006): Pre- and post-test mathematical modelling of a plan-asymmetric reinforced concrete frame building. *Earthquake Engineering and Structural Dynamics*, **35** (11), 1359-1379.

[19] Peruš I, Poljanšek K, Fajfar P (2006): Flexural deformation capacity of rectangular RC columns determined by the CAE method. *Earthquake Engineering and Structural Dynamics*, **35** (12), 1453-1470.

[20] CEN (2005): European standard EN 1998–3:2005. Eurocode 8: Design of structures for earthquake resistance. Part 3: Assessment and retrofitting of buildings, European Committee for Standardization, Brussels.

[21] Celarec D, Dolšek M (2013): Practice-oriented probabilistic seismic performance assessment of infilled frames with consideration of shear failure of columns. *Earthquake Engineering and Structural Dynamics*, **42** (9), 1339-1360.

[22] Žižmond J (2016): Force-based seismic design of reinforced concrete buildings for target reliability. *Ph.D. Dissertation* (in preparation), Faculty of Civil and Geodetic Engineering, University of Ljubljana.

[23] Chiou B, Darragh R, Gregor N, Silva W (2008) NGA Project Strong-Motion Database. *Earthquake Spectra*, **24** (1), 23-44.

[24] CEN (2004): European standard EN 1998–1:2004. Eurocode 8: Design of structures for earthquake resistance. Part 1: General rules, seismic action and rules for buildings. European Committee for Standardization, Brussels.

[25] Baker JW (2011): Conditional mean spectrum: Tool for ground-motion selection. *Journal of Structural Engineering*, **137** (3), 322-331.

[26] Jayaram N, Lin T, Baker JW (2011): A computationally efficient ground-motion selection algorithm for matching a target response spectrum mean and variance. *Earthquake Spectra*, **27** (3), 797-815.

[27] Liel AB, Haselton CB, Deierlein GG, Baker JW (2009): Incorporating modeling uncertainties in the assessment of seismic collapse risk of buildings. *Structural Safety*, **31** (2), 197-211.

[28] Brozovič M, Dolšek M (2014) Envelope-based pushover analysis procedure for the approximate seismic response analysis of buildings. *Earthquake Engineering and Structural Dynamics*, **43** (1), 77-96.